ELSEVIER

Journal of Alloys and Compounds 363 (2004) 292–298

Journal of ALLOYS AND COMPOUNDS

www.elsevier.com/locate/jallcom

Effects of rare-earth content and annealing on the electrochemical properties of $Mm(NiCoMnAl)_5$ hydrogen storage alloys

Rong Li*, Jianmin Wu, Shaoxiong Zhou, Xinlin Wang

Department of Functional Material Research, Center Iron and Steel Research Institute, Beijing 100081, China

Received 3 February 2003; received in revised form 6 May 2003; accepted 6 May 2003

Abstract

The effects of the La and Ce contents and heat treatment on the crystal structure and electrochemical properties of $Mm(NiCoMnAl)_5$ alloys were studied. For the as-cast alloy, the electrochemical capacity increases and cycle lifetime decreases with increasing La content. The lattice distortion and defects decreased and grain size increased for all the specimens studied after heat treatment. However, these alloys show very different electrochemical properties after heat treatment. For the La-rich alloys, the cycle lifetime increases obviously after heat treatment. But the electrochemical capacity decreases. Especially the high rate charge/discharge ability decreases markedly. For the Ce-rich alloys, both the electrochemical capacity and the cycle lifetime decreased after heat treatment.

Keywords: Rare earth compounds; Hydrogen absorbing materials; Electrode materials; Electrochemical reactions

1. Introduction

The rare earth-based hydrogen storage alloys have been used widely as cathode material of rechargeable Ni/MH batteries due to their high-energy density, high rate charge and discharge ability, long charge–discharge cyclic lifetime and environment compatibility [1–3].

The typical rare earth-based hydrogen storage alloy is $Mm(NiCoMnAl)_5$, in which Mm denotes mischmetal (a commercial mixture consist mainly of rare earth elements La, Ce, Pr, Nd). Nowadays, two kinds of mischmetal, namely La-rich and Ce-rich mischmetal owing to different mineral resources and extractive metallurgical methods, have been utilized widely in commercial hydrogen storage alloys. Several authors [4–10] have reported that the contents of La and Ce had a promising influence on the microstructure, hydrogen absorption–desorption properties and electrochemical characteristics such as lattice parameter, plateau pressure, electrochemical capacity, cycle lifetime and so on. Ohnishi et al. [7] reported that the electrochemical capacity of $MmNi_{4.0}Al_{0.3}Co_{0.7}$ increased linearly with increasing La content. Suzuki et al. [8] have studied the electrode properties of modified $MmNi_{4.0}Co_{0.6}Mn_{0.2}Al_{0.2}$ alloys by adding pure La, Ce and Nd into commercial Mm, and found that the initial electrochemical properties of these alloys depended largely on the original La content in Mm (expressed by La/Mm), because a higher La/Mm ratio results in lower hydrogen pressure. Lei et al. [9] discussed comprehensively the effect of the composition of rare earth elements (La, Ce, Pr, Nd) of mischmetal on the electrode properties. Also the relationship of cerium content and cycle life had been investigated in Ref. [5], and it was found that the rate of loss of electrochemical capacity per charge–discharge cycle due to electrode corrosion was significantly decreased due to the presence of Ce. Sakai et al. [4] pointed out the replacement of lanthanum by large amounts of cerium or neodymiun gave the alloy a satisfactory cycle lifetime even in the low content range of cobalt. In conclusion from these works, the element La is effective on the capacity and Ce is advantageous to cycle lifetime for as-cast alloys. However, different results were found for the La-rich and Ce-rich alloys both in electrochemical properties and microstructure after annealing.

It is well known that the conventional preparation of hydrogen storage alloys is ingot casting, and then the alloys are heat-treated normally to homogenize the segregated structure before pulverization. Several authors [11,12] indicated that the electrochemical capacity and cycling stability of

* Corresponding author. Tel./fax: +86-10-6218-3115.
E-mail address: lironghome@sina.com (R. Li).

0925-8388/$ – see front matter © 2003 Elsevier B.V. All rights reserved.
doi:10.1016/S0925-8388(03)00483-3

La-rich alloys were improved greatly after annealing due to enhancement of the compositional homogeneity and decrease of the lattice strain and defects. But Sakai et al. [4] reported that the annealed alloy, in which the mischmetal is comprised of 30%La, 52%Ce, 5%Pr, 13%Nd, showed a significant decrease in both capacity and cycle lifetime.

In this work, the phase structure and the electrochemical properties of $Mm(NiCoMnAl)_5$ both in as-cast and annealed alloys, which with different contents of La and Ce, were studied.

2. Experimental details

In this work three mischmetals were used, they are mischmetal-1 (32%La, 45%Ce), mischmetal-2 (42%La, 42%Ce) and mischmetal-3 (65%La, 22%Ce). Test samples of $MmNi_{3.65}Co_{0.75}Mn_{0.4}Al_{0.2}$ were conventionally casted by inductive melting a mixture of the composing elements under an argon atmosphere. The purity of all the elements is higher than 99.9%. According to the difference of the content of La and Ce, these alloys were marked as SS1#(Mm: 32%La, 45%Ce), SS2#(Mm: 42%La, 42%Ce) and SS3#(65%La, 22%Ce), respectively. The annealing treatment was performed at 1323 K for 8 h under 2×10^{-5} Torr vacuum. And then both as-cast and annealed alloys were crushed and ground mechanically to produce powder below 250 mesh for experiment.

X-ray diffraction analysis was carried out to identify the crystal structure of the specimens. Scanning electron microscopy (SEM) was used to observe the metallurgical microstructure.

For the electrochemical properties measurements, approximately 1 g of alloy powder was mixed with Ni powder, in a weight ratio of 1:1, and a small amount of polyvinyl alcohol solution as a binder, and then cold pressed to a pellet ($d=$ 15 mm) under 20 MPa used as the negative electrode. The counter electrode used was the same positive nickel electrode ($Ni(OH)_2$–NiOOH) as that employed in Ni–MH battery. The capacity of the counter-electrode was designed to be sufficiently large so that the capacity of the negative electrode was the limited capacity. The mercury oxide electrode (Hg/HgO/6 M KOH) was used as a reference electrode. In the experiment, the negative electrode was charged in 303

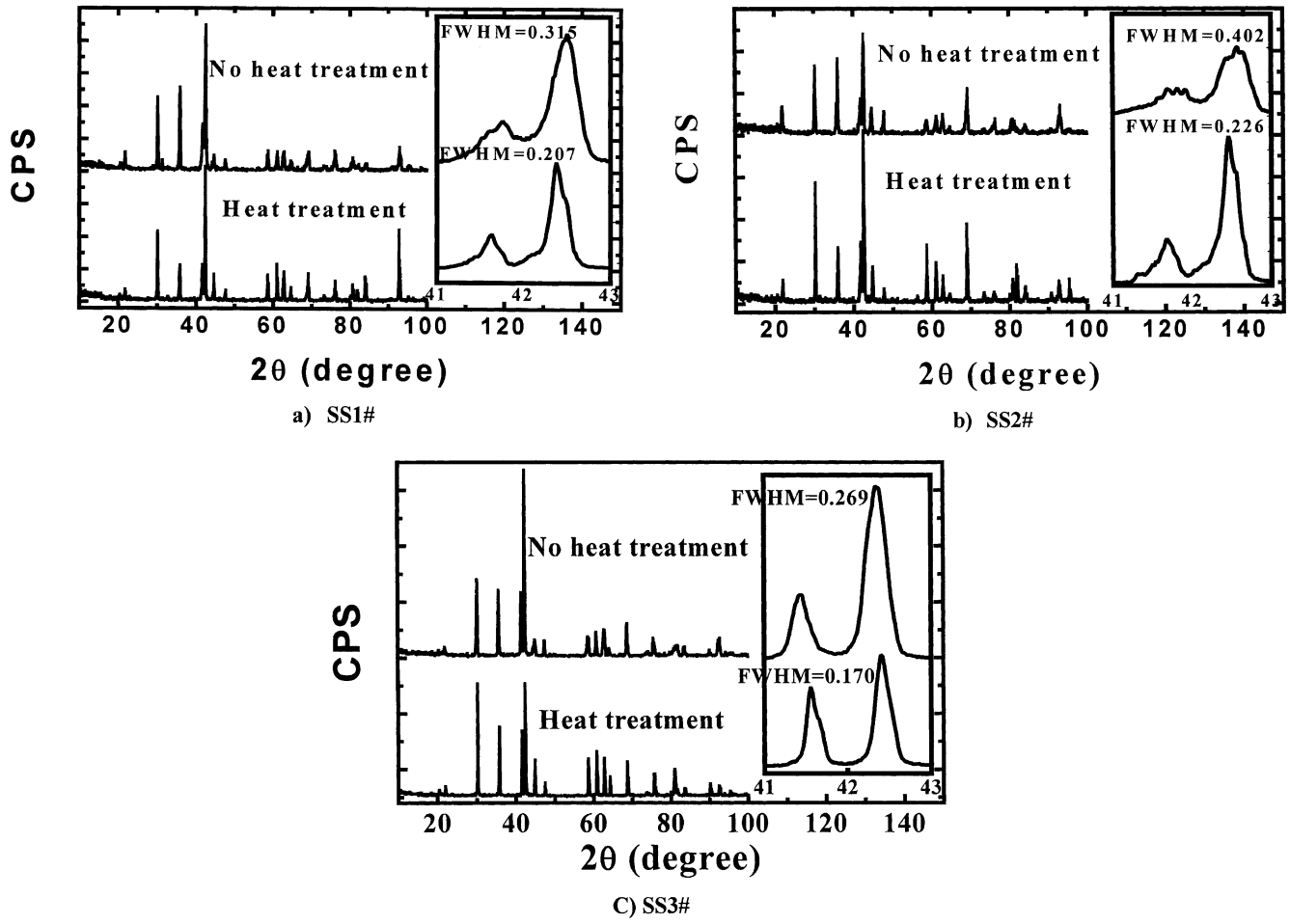

Fig. 1. X-ray diffraction results of all specimens (Cu target).

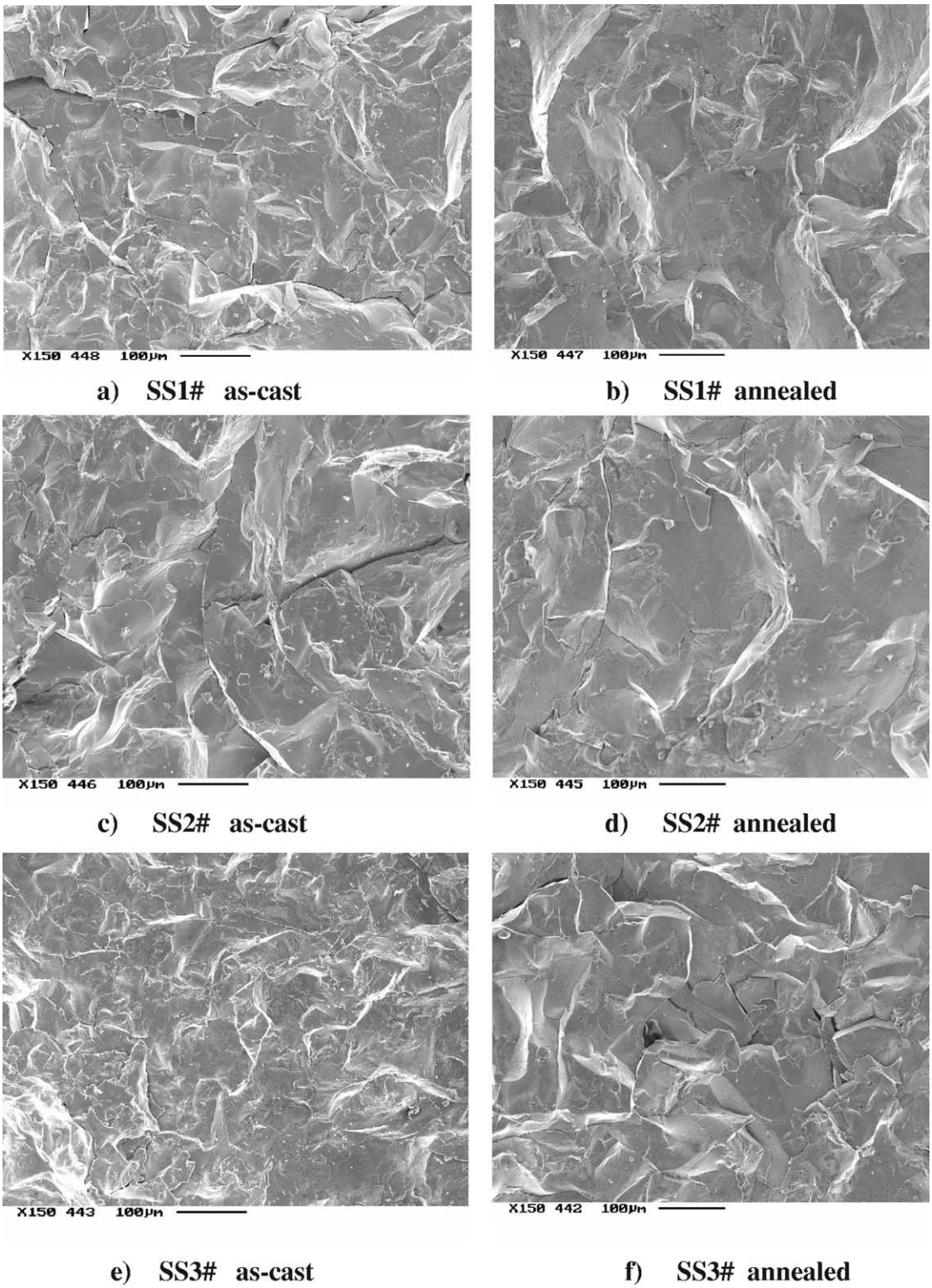

Fig. 2. SEM imagines of the metallurgical microstructure of rupture surfaces of SS1# as-cast (a), SS1# annealed (b), SS2# as-cast (c), SS2# annealed (d), SS3# as-cast (e) SS3# annealed (f).

K for 400 min at 60 mA/g, for 150 min at 150 mA/g or for 72 min at 300 mA/g current density, respectively, and after resting for 15 min, it was discharged to 0.5 V versus the Hg/HgO electrode, and after resting for 2 min, then it was charged again. For every sample, at first, it was charged and discharged at 60 mA/g current density. After utter activation, the test negative electrode was charged/discharged at 150 and 300 mA/g, respectively, to determine its electrochemical properties under different current densities. The cycle life experiment was carried out at 300 mA/g charge/discharge

current density. All the electrochemical measurement conditions were set and controlled by a computer, and the measuring dates were stored in the computer directly.

3. Results and discussion

3.1. Phase structure and metallurgical microstructure

The X-ray results of as-cast and annealed alloys, with different content of La and Ce, are shown in Fig. 1. Apparently, all the specimens exhibited a single-phase $CaCu_5$-type structure. Compared with the as-cast alloys, the positions of the Bragg diffraction peaks of the annealed alloys have slightly shifted. The peaks of SS1# and SS2# have shifted to smaller angles and that of SS3# shifted to the larger angles. This indicates that the lattice parameters of the alloys SS1# and SS2# have increased and the lattice parameters of the alloy SS3# have decreased after heat treatment. In addition, the width of diffraction peaks of all the specimens have become narrower and sharper after annealing. The full width at half-maximum (FWHM) of the (111) peak decreased from 0.315 to 0.207 for SS1#, from 0.402 to 0.226 for SS2# and from 0.269 to 0.170 for SS3# after annealing. It means that the lattice strain and defects, which were introduced into the alloy during casting, have been reduced [13,14], and that the particle size has increased during annealing. Moreover, the attainment of a more homogeneous composition of the dominant phase by annealing can also be considered as having narrowed the peak width. Fig. 2 shows the metallurgical microstructure of fracture surfaces of all the specimens. Compared with that of the as-cast alloys, a more integral character and larger grains can be observed in the annealed alloys.

3.2. Electrochemical properties

The maximum electrochemical capacities of all the specimens charged/discharged under different current density are summarized in Table 1. It can be noticed that corresponding to the previous reports [5,6,8], the capacity of as-cast alloys increases with increasing La content. According to Refs. [5,6,8], this capacity increase comes from the marked decrease of the hydrogen absorbing plateau pressure with increasing La content due to fact that the metal radius of La is larger than that of Ce, which results in increasing charge efficiency. It can be noticed from Table 1 that the electrochemical capacity of all the specimens decreases after heat treatment. These results are different from those of Ref. [11] for alloy SS3# but consistent with the results reported in Ref. [4] for the alloys SS1# and SS2#. Except the capacity, the more important property of hydrogen alloy is its cycle lifetime. According to Ref. [5], La is an important element for improving the capacity of an alloy, but Ce is a more important element for improving the cycle lifetime of an alloy. However, inversive results were obtained after annealing the samples.

Table 1
The maximum electrochemical capacities in different current density

Alloy no.	Sample	Capacity (mAh/g)		
		60 mA/g	150 mA/g	300 mA/g
S1#	As-cast	305	290	263
	Annealed	275	238	230
SS2#	As-cast	306	293	273
	Annealed	296	265	244
SS3#	As-cast	315	298	274
	Annealed	305	280	247

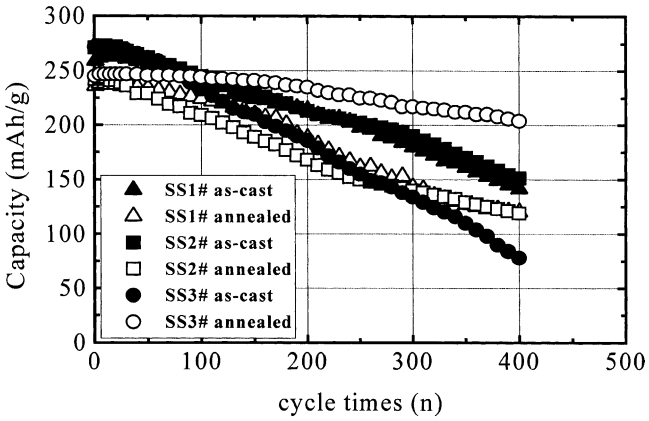

Fig. 3. Cycle lifetime measurement results of all specimens at 30 °C and 300 mA/g charge/discharge current density.

The cycle lifetime measurement results of both as-cast and annealed alloys under 300 mA/g rate charge/discharge condition are shown in Fig. 3. For the as-cast samples, conform to the result of reference [4,5,15,16], the cycle lifetime increases with increasing Ce content. However, the cycle lifetime of the Ce-rich alloy decreases and that of the La-rich alloy improves markedly after annealing.

It is well known that the potential variations during a cycle provide important information on the occurring processes. The potential hysteresis between the charging and discharging curves represent the uncompensated part of the ohmic resistance [1]. According to Ref. [1], the current density of electrode j is proportional to the specific area of the active electrode material:

$$j = \frac{i}{m \cdot \mathrm{SA}} \quad (1)$$

where m and SA are the mass (g) and the specific area ($cm^2\ g^{-1}$) of the active electrode material.

The relation between the current density j and the overpotential η can be described by the Tafel equation [17].

$$\eta = a + b \log j \quad (2)$$

where a and b are the Tafel constants.

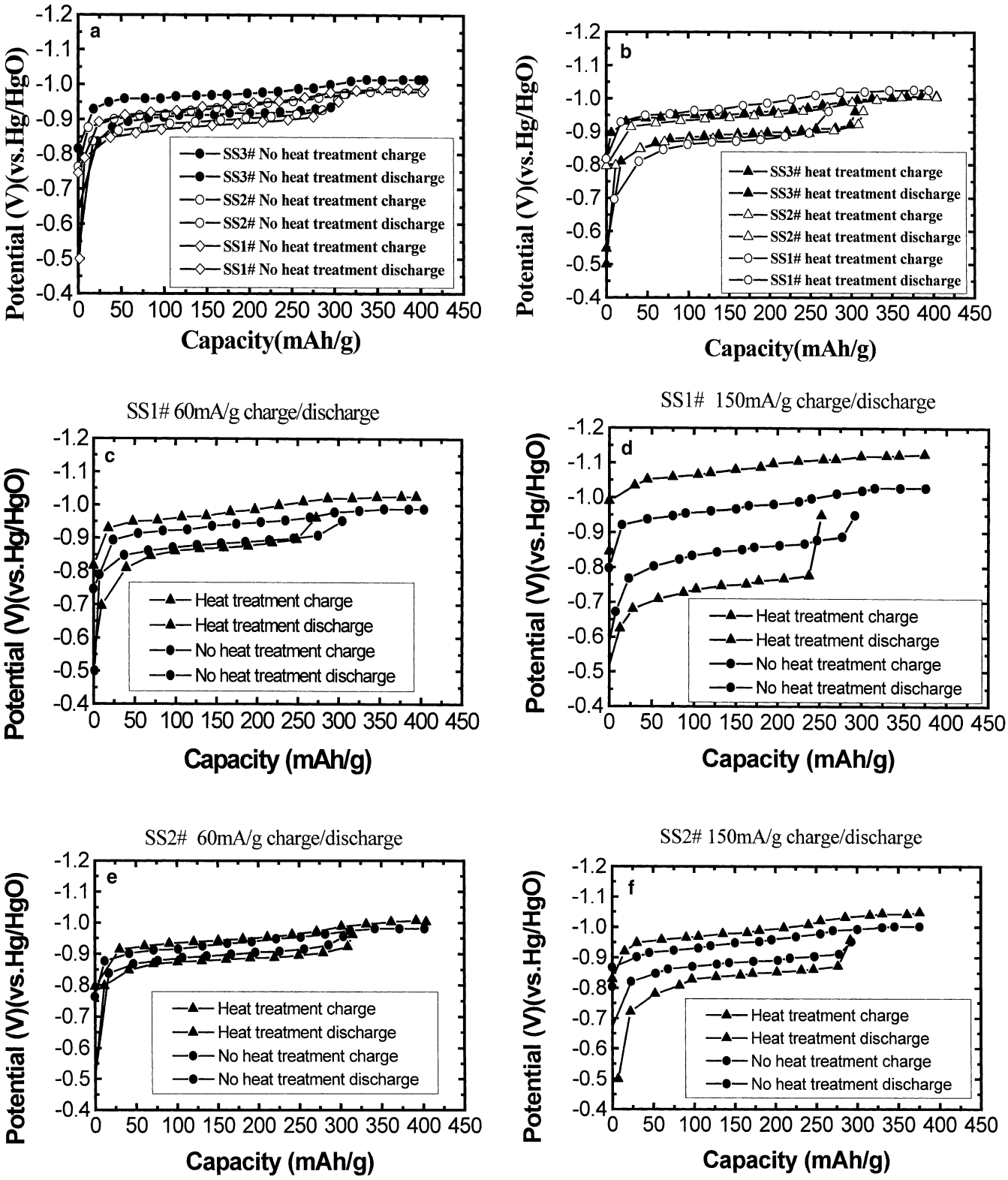

Fig. 4. Tenth cycle charge/discharge curves under 60 mA/g rate and fifth cycle charge/discharge curves under 150 mA/g rate after charge/discharge under 60 mA/g rate of the as-cast and annealed samples. (a) Tenth cycle charge/discharge curves under 60 mA/g rate of SS1#, SS2# and SS3# as-cast samples. (b) Tenth cycle charge/discharge curves under 60 mA/g rate of SS1#, SS2# and SS3# annealed samples. (c) Tenth cycle charge/discharge curves under 60 mA/g rate of SS1# as-cast and annealed samples. (d) Fifth cycle charge/discharge curves under 150 mA/g rate after charge/discharge under 60 mA/g rate of SS1# as-cast and annealed samples. (e) Tenth cycle charge/discharge curves under 60 mA/g rate of SS2# as-cast and annealed samples. (f) Fifth cycle charge/discharge curves under 150 mA/g rate after charge/discharge under 60 mA/g rate of SS2# as-cast and annealed samples. (g) Tenth cycle charge/discharge curves under 60 mA/g rate of SS3# as-cast and annealed samples. (h) Fifth cycle charge/discharge curves under 150 mA/g rate after charge/discharge under 60 mA/g rate of SS3# as-cast and annealed samples.

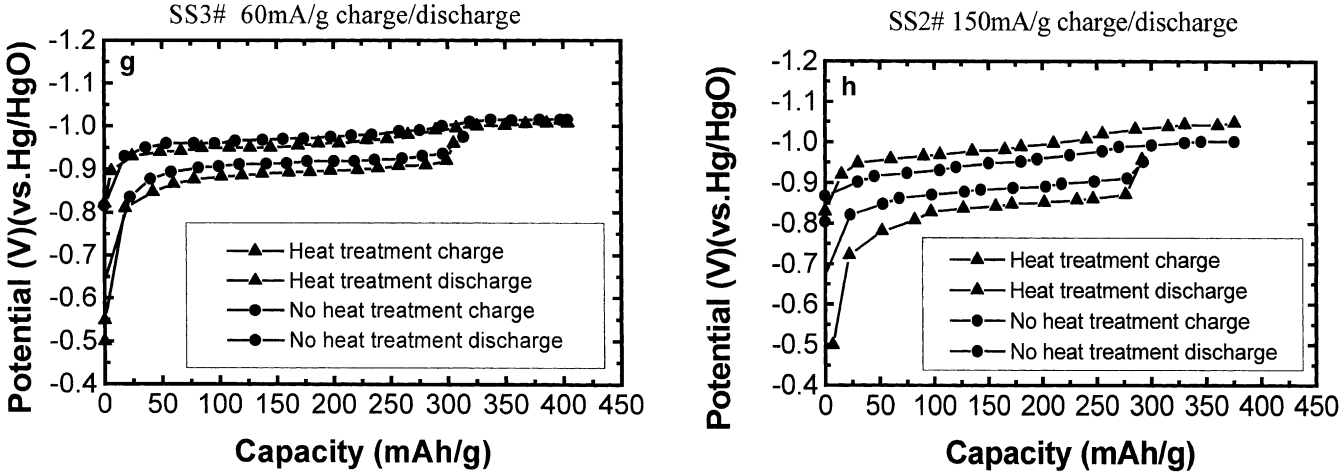

Fig. 4. (*Continued*).

The tenth cycle of the charge/discharge curves under 60 mA/g rate and the fifth cycle of the charge/discharge curves under 150 mA/g rate after charge/discharge under 60 mA/g rate of the as-cast and annealed samples are shown in Fig. 4. For the as-cast alloys, it can be noticed from Fig. 4a that the charge/discharge overpotential and the potential hysteresis of the La-rich alloy are larger than that of the Ce-rich alloys. According to Eqs. (1) and (2), the specific area of the La-rich alloy is smaller than that of the Ce-rich alloys. It can be concluded that the particle size of the La-rich alloy is larger than that of the Ce-rich alloys due to the fact that the specific area of an electrode material is inversely proportional to the particle size. After annealing, the charge/discharge overpotential and the potential hysteresis of the Ce-rich alloys increase and are larger than that of La-rich alloy as shown in Fig. 4b. From Fig. 4c–f it can be inferred that annealing results in a marked increase of the overpotential of the Ce-rich alloy. Especially for the high rate 150 mA/g charge/discharge, a large hysteresis was found between the charge/discharge electrode potential curves for the Ce-rich alloy. This result is consistent with that of Ref. [18] and the hysteresis decreases with increasing La content. The charge/discharge curve of the annealed alloys is nearly the same as that of the as-cast alloy for the La-rich samples under 150 mA/g charge/discharge condition. It shows that the particle size of the Ce-rich alloys has increased more than that of the La-rich alloys during annealing.

It is well known that the particles will expand and shrink during the charge and discharge process due to absorption and desorption of hydrogen atoms. This expanding and shrinking will result in particle pulverization. Much more particle pulverization will occur alloys with larger particle size. From the analysis given above, it can be derived that the particle size of the Ce-rich alloys is smaller than that of the La-rich alloys before annealing and has strongly increased after annealing.

In Ref. [19] it was demonstrated that cerium forms a close packed face centered cubic structure, in contrast to all other rare earth metals, which form a less dense hexagonal structure [20]. This means that for some reason cerium has a higher ‘packing capability’ than La, Pr or Nd. So Ce is the most effective in increasing the structural anisotropy (expressed by the lattice parameter ratio: c/a), which may lead to the highest corrosion stability, but it also increases the plateau pressure most significantly, which in turn reduces the capacity. On the other hand, another difference between Ce and La, Pr or Nd is that Ce can exist in states of mixed valency [21]. Ce can form a protective oxide film on metal surfaces and it has been shown via XANES studies that Ce in the film is tetravalent and present as CeO_2 [15,16]. Sakai et al. [4] indicated that the surface layer of the crystal grain played a very important role in preventing capacity decay for Ce-rich alloys. Due to the protective layer formed on the grain boundaries, the protective ability would be effective until the alloy was pulverized below the grain size. So it is expected that the alloy with the smaller grain size has a longer cycle lifetime for the Ce-rich alloys. From this analysis we can understand why the cycle lifetime of the Ce-rich alloys decreases after annealing.

As for the La-rich alloy SS3#, the particle size has only slightly increased after annealing according to the analysis above. This increase in particle size results in a decrease of the specific area and capacity, especially in a decrease of the high rate charge/discharge ability. Moreover, La is easily oxidized to $La(OH)_3$ or La_2O_3, which has been observed in Ref. [22]. These factors are responsible for the deterioration in cycle durability for the as-cast alloy. Willems and Buschow [23] reported that diffusion of lanthanum atoms to the surface area should be prevented so as to decrease volume expansion and increase the cycle lifetime, so we think that the La in the grain surface will diffuse into the inner part leading to a more homogeneous

composition of the alloy during the heat treatment process. This phenomenon will lessen the lattice expansion and oxidization of the La and improve the cycle lifetime of the alloy. Also the decrease of the lattice strain and defects after annealing plays a very important role on the cycle stability, because lattice strain and defects will result in pulverization of the particles during the charge/discharge process.

4. Conclusions

The effects of the La and Ce contents and heat treatment on the crystal structure and electrochemical properties of $Mm(NiCoMnAl)_5$ alloys were studied. For the as-cast alloy, the electrochemical capacity increases and cycle lifetime decreases with increasing La content. The lattice distortion and defects decreased and the grain size increased after heat treatment in all the specimens studied. However, these alloys show very different electrochemical properties after heat treatment. For the La-rich alloys, the cycle lifetime increased obviously after heat treatment. But the electrochemical capacity decreases. Especially the high rate charge/discharge ability decreases markedly. The electrochemical capacity decrease for the La-rich alloys after annealing is ascribed to an increased particle size and a decreased specific area. The cycle lifetime increase of the La-rich alloys after annealing is ascribed to a more homogeneous composition and to a decrease of the lattice distortion and defects.

For the Ce-rich alloys, both the electrochemical capacity and the cycle lifetime decreased after heat treatment. This decrease is thought to come from the marked increase of the particle size of the alloys after annealing.

Acknowledgements

This work was supported by the National 863 project (No.: 2002AA323070), from the Ministry of Science and Technology, China.

References

[1] J.J.G. Willems, Philips J. Res. 39 (1984) 1.
[2] T.N. Veziroglo, Int. J. Hydrogen Energy 1 (1987) 99.
[3] T. Sakai, H. Miyamura, N. Kuriyama, A. Kato, K. Oguro, H. Ishikawa, J. Electrochem. Soc. 137 (1990) 795.
[4] T. Sakai, T. Hazama, H. Miyamura, N. Kuriyama, A. Kato, H. Ishikawa, J. Less-Common Metals 172–174 (1991) 1175.
[5] G. Adzic, J.R. Johnson, J.J. Reilly, J. McBreen, S. Mukerjee, M.P.S. Kumar, W. Zhang, S. Srinivasan, J. Electrochem. Soc. 142 (1995) 3429.
[6] G. Adzic, J.R. Johnson, S. Mukerjee, J. McBreen, J.J. Reilly, J. Alloys Comp. 253/254 (1997) 579.
[7] M. Ohnishi, Y. Matsumura, K. Hasegawa et al., Abstr. 33rd National Japanese Semin. on Batteries, 1992, p. 163.
[8] K. Suzuki, N. Yanagihara, H. Kawano, A. Ohta, J. Alloys Comp. 192 (1993) 173.
[9] Y. Lei, J. Jiang, D. Sun, J. Wu, Q. Wang, J. Alloys Comp. 231 (1995) 553.
[10] V.Z. Mordkovich, Yu.K. Baichtok, N.V. Dudakova, E.I. Mazus, V.P. Mordovin, J. Alloys Comp. 231 (1995) 498.
[11] W.-K. Hu, K.-M. Kim, S.-W. Jeon, J.-Y. Lee, J. Alloys Comp. 270 (1998) 255.
[12] J.H. Guo, Z.T. Jiang, Q.S. Duan, G.Z. Liu, J.H. Zhang, C.M. Xia, S.Y. Guo, J. Alloys Comp. 293–295 (1999) 821.
[13] K. Nomuram, H. Uruno, S. Ono, H. Shinozuka, S. Suda, J. Less-Common Met. 107 (1985) 221.
[14] E.H. Kisi, C.E. Buckley, E.M. Gray, J. Alloys Comp. 185 (1992) 369.
[15] A.J. Davenport, H.S. Isaacs, M.W. Kendig, Corrosion Sci. 32 (1991) 653.
[16] S. Mukerjee, J. McBreen, J.J. Reilly, J.R. Johnson, G. Adzic, K. Petrov, M.P.S. Kumar, W. Zhang, S.J. Srinivasan, J. Electrochem. Soc. 142 (1995) 2278.
[17] A.J. Bard, L.R. Faulkner, in: Electrochemical Methods, Wiley, New York, 1980.
[18] M.N. Mungole, R. Balasubramaniam, K.N. Rai, K.P. Singh, Int. J. Hydrogen Energy 17 (1992) 603.
[19] L.O. Valøen, A. Zaluska, L. Zaluski, H. Tanaka, N. Kuriyama, J.Q. Ström-Olsen, R. Tunold, J. Alloys Comp. 306 (2000) 235.
[20] G.H. Ayward, T.J.V. Findlay, in: SI Chemical Data, 2nd Edition, Wiley, Australia, 1974.
[21] F. Lopez-Aguilar, J. Costa-Quintana, M. Sanchez-Lopez, Phys. Rev. B 56 (3) (1997) 1335.
[22] L. Schlapbach, A. Seiler, F. Stucki, H.C. Siegmann, J. Less-Common Met. 73 (1980) 145.
[23] J.J.G. Willems, K.H.J. Buschow, J. Less-Common Met. 129 (1987) 13.